Characteristics and Effects on Dental Pulp Cells of a Polycaprolactone/Submicron Bioactive Glass Composite Scaffold

Sainan Wang, PhD, Qing Hu, PhD,† Xuejun Gao, PhD,* and Yanmei Dong, PhD**

Abstract

Introduction: This study aimed to evaluate the potential applications of polycaprolactone (PCL)/submicron bioactive glass (smBG) hybrid composites for pulp and dentin tissue regeneration. **Methods:** PCL/smBG hybrid composites were made with novel monodispersive bioactive glass submicrospheres, and pure PCL and bioactive glass samples were used as controls. Surface characteristics were assessed by scanning electron microscopy. Crystalline apatite deposition *in vitro* was examined after incubation in simulated body fluid. Inductively coupled plasma spectroscopy was used to further analyze the concentration of Si ions released by the scaffolds. Cell adhesion and morphology of human dental pulp cells were observed by immunofluorescence staining. The proliferation and expression of odontogenic-related markers were subsequently investigated using the Cell Counting Kit-8 assay (Beyotime Institute of Biotechnology, Jiangsu, China), Western blotting, and real-time reverse-transcription polymerase chain reaction. Mineralization activity was assessed by alizarin red staining. **Results:** Crystalline apatites were precipitated on the PCL/smBG hybrid and pure bioactive glass surfaces after incubation *in vitro*, and pure PCL did not exhibit precipitation. Surface deposition on PCL/smBG hybrids presented different topographies and was thicker than on pure bioactive glass scaffolds at a later stage. Human dental pulp cells had a significantly higher proliferation rate on the PCL/smBG hybrid than on the bioactive glass and PCL scaffolds. Furthermore, the integration of smBG into the hybrid scaffold significantly promoted the expression of markers for odontogenic differentiation. More mineralized nodules were generated in the PCL/smBG group than in the other 2 groups. **Conclusions:** PCL/smBG hybrid composites may serve as potential material for pulp repair and dentin regeneration. The physical and chemical properties of the bioactive glass component affect the bioactivity of hybrid composites. *(J Endod 2016;42:1070–1075)*

Key Words

Bioactive glass, odontogenic differentiation, polycaprolactone, tooth engineering

Significance

Polycaprolactone/submicron bioactive glass hybrid composites significantly enhance proliferation and differentiation of human dental pulp cells and might be suitable scaffolds for tooth engineering. The mineralization ability and bioactivity of the composites can be affected by bioactive glass component.

As a biodegradable bioceramic material, bioactive glass (BG) can directly affect osteogenic gene expression and has been used for bone regeneration (1). Our previous study showed that BG facilitates odontogenic differentiation and dentin formation of dental pulp cells, suggesting that it is potentially useful for tooth engineering (2, 3). However, BG has poor mechanical properties, such as high brittleness and low tensile strength, which primarily restrict its practical application in scaffolds for dental tissue engineering.

Scaffolds that combine BG with natural or synthetic organic polymers, such as collagen or polycaprolactone (PCL), exhibit good properties and biological activity in bone tissue engineering (4–6). However, unlike bone tissue, the dental-pulp complex offers the unique and functional structure of the tooth. In this complex, the odontoblast cells and the pulp are located at one side of the mineralized dentin where no cells are entrapped in the matrix. Recently, researchers have developed a gelatin/BG hybrid porous scaffold and a collagen/BG membrane for dentin/pulp regeneration, confirming the positive biological effects of BG composites on odontogenic responses (7, 8). However, the structures of these composites resemble those used in bone repair. Scaffolds that provide a suitable interface for cellular activity and tissue regeneration upon, but not inside, the scaffolds may better facilitate pulp and dentin engineering. In addition, little information is available regarding the effects of the BG component in the composites on the mineralization characteristics and odontogenic activity. Based on this concept, we sought to develop a composite scaffold made with novel submicron BG (smBG) incorporated with PCL.

The aim of this study was to investigate whether the PCL/smBG hybrid composites provide a suitable microenvironment for the odontogenic transformation of human dental pulp cells (hDPCs) and to further evaluate the effect of the novel smBG component on the biological performance of hybrid scaffolds.

From the *Department of Cariology and Endodontology, Peking University School and Hospital of Stomatology, Beijing, People's Republic of China; and †National Engineering Research Center for Tissue Restoration and Reconstruction, South China University of Technology, Guangzhou, People's Republic of China.

Address requests for reprints to Dr Yanmei Dong, Peking University School and Hospital of Stomatology, Department of Cariology and Endodontology, 22 Zhongguancun Nandajie, Haidian District, Beijing 100081, China. E-mail address: kqdongyanmei@bjmu.edu.cn

0099-2399/$ - see front matter

http://dx.doi.org/10.1016/j.joen.2016.04.023

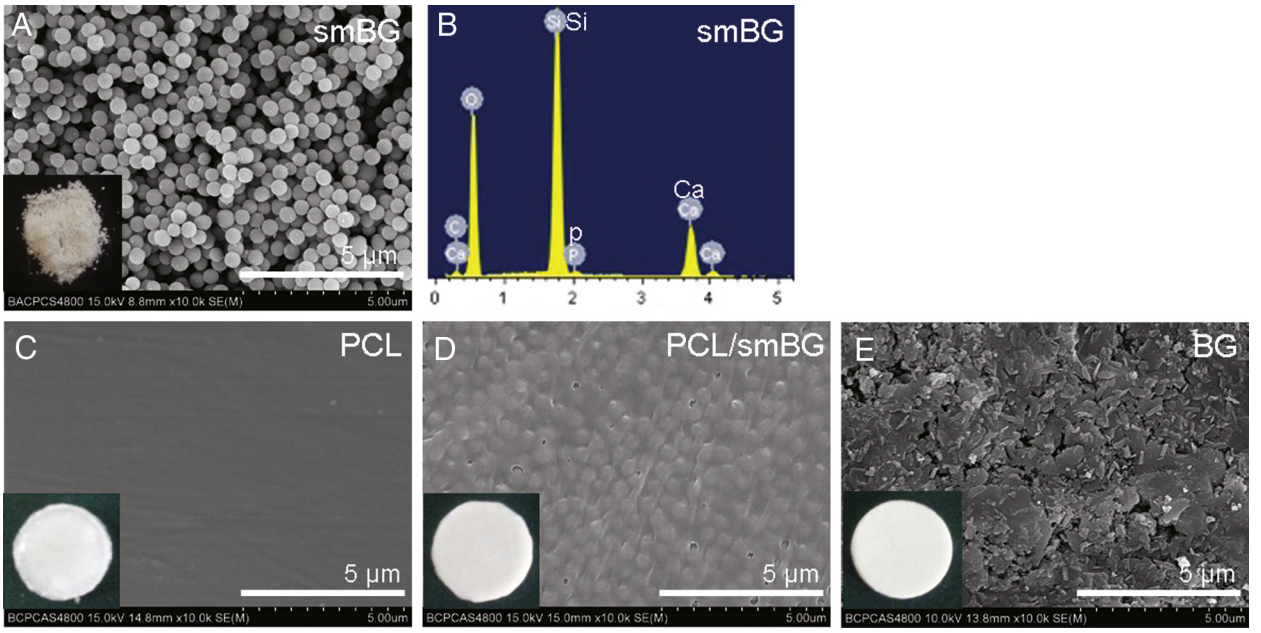

Figure 1. Surface morphology and elemental composition of smBG and scaffolds. (*A*) Surface morphology of smBG, (*B*) surface elemental composition of smBG, (*C*) surface morphology of pure PCL scaffolds, (*D*) PCL/smBG hybrid scaffolds, and (*E*) pure BG scaffolds.

Materials and Methods

Preparation of Scaffolds

PCL/smBG hybrid composites were produced by combining the conventional solvent casting technique and the thermal pressing method. First, smBG was synthesized according to a previous publication (9). smBG exhibited a regular spherical morphology and a relatively narrow particle size distribution (510–590 nm) with a mean diameter of 560 nm. These particles had favorable monodispersibility (Fig. 1*A*). The energy disperse X-ray spectra showed that the surfaces of the smBG were composed of large amounts of silicon (Si), some calcium (Ca), and phosphate (P) (Fig. 1*B*); the analysis of the relative intensity of these peaks indicated the molar ratio of Si:Ca:P was 77:20:3. Then, the smBG particles (60 wt% in relation to the PCL) were ultrasonically dispersed into 10 mL tetrahydrofuran solvent, and the PCL polymers were added with magnetic stirring for 10 hours. The prepared mixture was then poured into glass Petri dishes and kept at room temperature for 24 hours to remove the solvent. After this stage, the composites were dried under a vacuum for 24 hours to completely remove residual liquid phases. Finally, the composites were heated at 37°C for 10 minutes and then pressed into PCL/smBG composite scaffolds. Pure PCL scaffolds prepared similarly but without adding BG and pure BG scaffolds sintered from 45S5 BG powder were used as controls.

Scanning Electron Microscopy

The surface morphology and microstructure of the scaffolds were characterized using a field emission scanning electron microscope (S4800; JEOL, Tokyo, Japan). The fields were selected randomly.

Apatite-forming Bioactivity Test

Each specimen was immersed in simulated body fluid (SBF) at an initial pH of 7.40 and placed in an orbital shaker at a constant speed of 120 rpm at 37°C for 1 day or 5 days. Then, scaffolds were rinsed 3 times in ethanol and deionized water and dried overnight at 37°C. The morphology of the hydroxyapatite layer on the scaffold surface was evaluated using scanning electron microscopy. The fields were selected randomly.

Inductively Coupled Plasma Spectroscopy

The samples were immersed in 2 mL phosphate-buffered saline (PBS) at 37°C for 1 day and 5 days. The release of silicon ions from the samples was measured by inductively coupled plasma optical emission spectroscopy (Vista-Pro Axial; Varian Inc, Palo Alto, CA). Three individual experiments were performed.

Cell Culture

hDPCs were derived from impacted fully developed healthy intact human third molars that were collected from 19- to 25-year-old patients at the Oral Surgery Department of Peking University School and Hospital of Stomatology, Beijing, People's Republic of China, after informed consent and ethics permission (reference no. PKUSSIRB-2013014) were obtained (2). hDPCs were cultured in sterile regular medium (Dulbecco modified Eagle medium; Gibco, Gaithersburg, MD) supplemented with 10% fetal bovine serum (HyClone, Piscataway, NJ), 100 U/mL penicillin, and 100 μg/mL streptomycin at 37°C in 5% CO_2. hDPCs at passages 3 to 5 were used for further experiments. The PCL/smBG hybrid and pure BG and PCL scaffolds were separately placed into the wells of 24 six-well plates and sterilized using ultraviolet light for 1 hour. hDPCs were seeded into the wells; after incubation at 37°C for 4 hours, the scaffolds containing cells on their surfaces were transferred into new plates for further experiments.

Cell Immunofluorescence Staining

hDPCs were seeded onto the scaffolds at 5×10^4 cells/scaffold. After 1 day of culture, the scaffolds were washed twice and fixed in 4% paraformaldehyde. Rhodamine phalloidin (160 nmol/L; Cytoskeleton Inc, Denver, CO) was used to stain the cellular cytoskeleton. After 5 days of culture, acridine orange staining was used to show the living cells. The staining results were observed under a confocal laser

TABLE 1. Forward and Reverse Primers for Reverse-transcription Polymerase Chain Reaction

Gene	GenBank no.	Sequences (5′–3′)	Size (bp)
DMP-1	NM_004407.3	Forward: AGGAAGTCTCGCATCTCAGAG Reverse: TGGAGTTGCTGTTTTCTGTAGAG	100
DSPP	NM_014208.3	Forward: ATATTGAGGGCTGGAATGGGGA Reverse: TTTGTGGCTCCAGCATTGTCA	136
RUNX2	NM_001024630.3	Forward:TCTTAGAACAAATTCTGCCCTTT Reverse: TGCTTTGGTCTTGAAATCACA	136
GAPDH	NM_002046.3	Forward: GAAGGTGAAGGTCGGAGTC Reverse: GAGATGGTGATGGGATTTC	225

DMP-1, dentin matrix protein 1; DSPP, dentin sialophosphoprotein; GAPDH, glyceraldehyde-3-phosphate dehydrogenase; RUNX2, runt-related transcription factor 2.

scanning microscope (FV1000; Olympus, Tokyo, Japan). The pictures were taken randomly.

Cell Counting Kit Assay

hDPCs (5×10^4) were seeded onto the scaffolds. After 2 and 5 days of culture, cell proliferation was evaluated using the Cell Counting Kit-8 (Beyotime Institute of Biotechnology, Jiangsu, China) according to the manufacturer's instructions. The absorbance was determined at 450 nm with a reference wavelength of 630 nm. Three individual experiments were performed, and each sample was conducted in quadruplicate.

Western Blot

Specimens were put into the upper compartment of transwell chambers, and hDPCs (5×10^4) were seeded into the lower compartment; the pore polycarbonate membranes allowed the interchange of chemical species between the upper and lower chambers. After 7 days of culture, the culture plates with hDPCs and extracellular matrices in the lower compartment were collected. Exactly 30 μg proteins per lane was loaded onto sodium dodecyl sulfate polyacrylamide gel electropheresis (SDS-PAGE) gels for electrophoresis and then transferred onto polyvinylidene fluoride (PVDF) membranes (Millipore Co, Bedford, MA). The membranes were blocked and then incubated overnight at 4°C with monoclonal antibody against collagen I (1:400; Abcam, Cambridge, MA), dentin sialophosphoprotein (DSPP, 1:400; Santa Cruz Biotechnology, Santa Cruz, CA), and glyceraldehyde-3-phosphate dehydrogenase (GAPDH, 1:1000; Zhongshan, Beijing, China). Afterward, the membranes were incubated with appropriate horseradish peroxidase–conjugated secondary antibodies at 1:5000 (Santa Cruz) at room temperature for an additional hour. The membranes were then visualized by chemiluminescence (Millipore Co) and exposed using the ChemiDoc XRS System (Bio-Rad, Hercules, CA). GAPDH served as an internal control.

Real-time Reverse-transcription Polymerase Chain Reaction. hDPCs (5×10^4) were seeded onto the scaffolds. After 3 and 7 days of culture, total RNA was isolated using Trizol reagent (Vigorous Biotech, Beijing, China) according to the manufacturer's instructions. Complementary DNA synthesis was performed in a 25-μL reaction mixture containing 2 μg total RNA, 400 mmol/L reverse-transcription primers, 4 U/μL Moloney murine leukemia virus (M-MLV), 1 U/μL ribonuclease inhibitor (RNasin), and 0.4 mmol/L deoxy-ribonucleotide triphosphate (dNTP) mix using M-MLV reverse transcriptase (Promega, Madison, WI). The amplification reaction was performed in an ABI 7300 Real-time PCR System (Applied Biosystems, Foster City, CA) with SYBR Green Master Mix (Toyobo, Osaka, Japan) and the appropriate primers (Table 1). Real-time reverse-transcription polymerase chain reaction conditions were as follows: 95°C for 10 minutes followed by 40 cycles at 95°C for 15 seconds and 60°C for 1 minute. The results were calculated from 3 independent experiments.

Alizarin Red Staining. hDPCs (5×10^4) were seeded onto the scaffolds. After 4 weeks of culture, the scaffolds were washed with PBS, fixed in 4% formaldehyde at room temperature for 15 minutes, and then stained with 1 mL alizarin red (0.1%; Sigma-Aldrich, St Louis, MO) for 30 minutes. Then, samples were washed with distilled water to remove any unincorporated alizarin red. Images were acquired using a scanner. Three individual experiments were performed.

Statistics

Results are expressed as the mean ± standard deviation. An independent sample *t* test was performed, and *P* values <.05 were considered statistically significant.

Results

Surface Characteristics of Scaffolds

All synthetic scaffolds were white disks ~10 mm in diameter and 1 mm in thickness. Scanning electron microscopy indicated that the PCL scaffolds had a smooth surface, whereas the PCL/smBG hybrid scaffolds exhibited an interconnected structure of homogeneous spherical particles interspersed within the PCL matrix. The pure BG scaffolds were coarser than the other samples (Fig. 1*C*–*E*).

In Vitro Mineralization Bioactivity of Scaffolds

A crystalline structure precipitated on the surfaces of PCL/smBG and pure BG scaffolds after incubation in SBF for 1 day and 5 days (Fig. 2*A*). However, pure PCL did not exhibit precipitation apatite crystals after up to 5 days of incubation. On day 1, the topographies of apatite precipitation on PCL/smBG and pure BG scaffolds differed. The apatite on the surface of the PCL/smBG hybrids presented small spherical structures, whereas a relatively flat layer of apatite covered the pure BG scaffolds. Under high magnification, the apatites on the 2 groups were both composed of similar interconnected reticular crystallites. On day 5, the apatite on PCL/smBG became flatter than on day 1. The topologies of the apatite on the pure BG scaffolds on day 5 were similar to that noted on day 1.

Cross-sectional images of truncated specimens showed that the thickness of the apatite layer on the PCL/smBG scaffolds increased significantly from 3.5 μm on day 1 to 19 μm on day 5, whereas the precipitation on BG scaffolds was 4 μm on day 1 and 8 μm on day 5 (Fig. 2*B*).

Ion Release Characteristics of Scaffolds

The Si concentration in the PBS solution was lower in the PCL/smBG hybrid group than in the pure BG group on 1 day ($P < .05$). On day 5, the Si concentration released by the PCL/smBG hybrids increased and did not significantly differ from pure BG. In

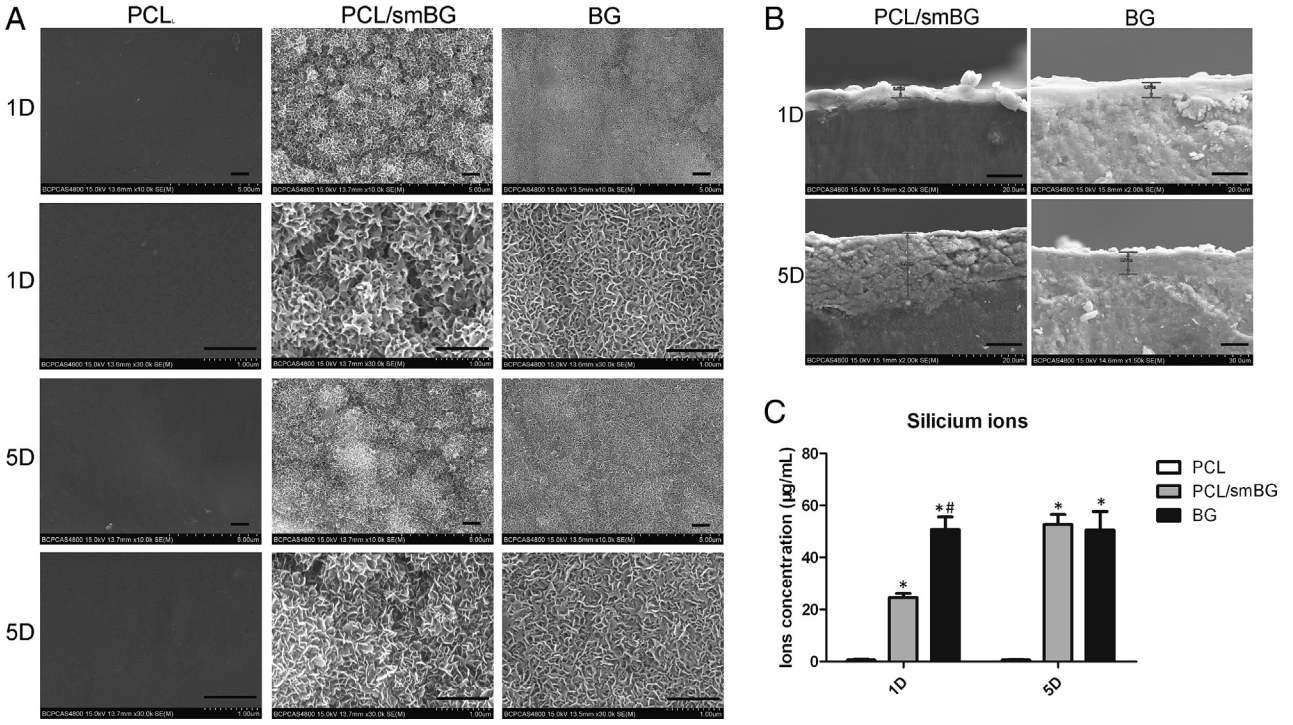

Figure 2. *In vitro* mineralization bioactivity and ion release characteristics of scaffolds. (*A*) Scanning electron microscopic micrographs showing the precipitation of apatite crystals on PCL/smBG hybrid scaffolds and pure BG scaffolds after incubation in simulated body fluid for 1 day and 5 days (scale bar = 1 μm). (*B*) The thickness of the apatite layer on the PCL/smBG scaffolds and pure BG control disks (scale bar = 10 μm). (*C*) Si ion released by pure and PCL/smBG hybrid scaffolds over time as detected by inductively coupled plasma spectroscopy. *Significant differences between the PCL/smBG or BG group and the PCL group ($P < .05$). #Significant differences between the PCL/smBG group and the BG group ($P < .05$).

the control PCL groups, the amount of Si ions on days 1 and 5 was negligible (Fig. 2*C*).

Viability, Distribution, and Morphology of hDPCs on Scaffolds

hDPCs on all samples showed an elongated, spindle-shaped morphology after 1 day of culture as assessed by rhodamine phalloidin staining (red). On day 5, amounts of live cells covered all the scaffolds based on acridine orange staining (yellowish-green) (Fig. 3*A*).

Proliferation of hDPCs on Scaffolds

On day 2, the Cell Counting Kit-8 showed no significant differences among the 3 groups. hDPCs in all groups showed an increasing proliferative tendency during 5 days of culture. On day 5, the values in the PCL/smBG hybrid group were significantly higher than in the other groups, and the lowest value was noted in the PCL group (Fig. 3*B*).

Odontogenic Differentiation of hDPCs on Scaffolds

Real-time reverse-transcription polymerase chain reaction results revealed a statistically significant increase in dentin matrix protein 1 (DMP-1) gene expression in hDPCs cultured with PCL/smBG compared with the other 2 groups at both 3 and 7 days. DSPP and runt-related transcription factor 2 (RUNX2) expression in the PCL/smBG groups was stronger than those in the other 2 groups on day 3. On day 7, DSPP and RUNX2 in the BG groups also increased but were not significantly different from those in the PCL/smBG group (Fig. 3*C*).

Odontogenic-related proteins were tested. After 7 days in culture, collagen I expression in the PCL/smBG group was increased compared with the PCL and BG groups, whereas DSPP expression was enhanced in the PCL/smBG and BG groups compared with the PCL group (Fig. 3*D*).

Alizarin red staining revealed that more mineralized nodules were generated in the PCL/smBG group than in the other 2 groups after 4 weeks of culture (Fig. 3*E*).

Discussion

Calcium silicone–based materials, such as iRoot (Innovative Bioceramix Inc, Vancouver, Canada), mineral trioxide aggregate (MTA, Dentsply Tulsa Dental, Tulsa, OK), and BioAggregate (Innovative BioCeramix), showed good cell biocompatibility and odontogenic-inducing ability in endodontic application (10–12). BG is a type of degradable bioceramic material and may serve as a good candidate scaffold for tooth engineering.

The smBG obtained by the improved sol-gel method in this study exhibited favorable monodispersibility, which solves the agglomeration problem of conventional sol-gel BG. Previous studies have shown that regular spherical BG exhibits better physicochemical and biological properties than irregular BG (13). The novel structure and properties of smBG may also make it a good drug or protein carrier (9, 14, 15). In this study, the well-defined morphology and monodispersibility of smBG particles allowed them to be dispersed uniformly in the PCL matrix, making it easier to control ion release from the composites than with irregular BG. In the apatite-forming bioactivity test, the crystallites on PCL/smBG hybrids formed small balls, and the size and contour of these balls were consistent with smBG particles. This finding indicated that the distribution and morphology of BG in the composites affect the *in vitro* mineralization process, suggesting that mineralization may be regulated by controlling the BG in composite materials.

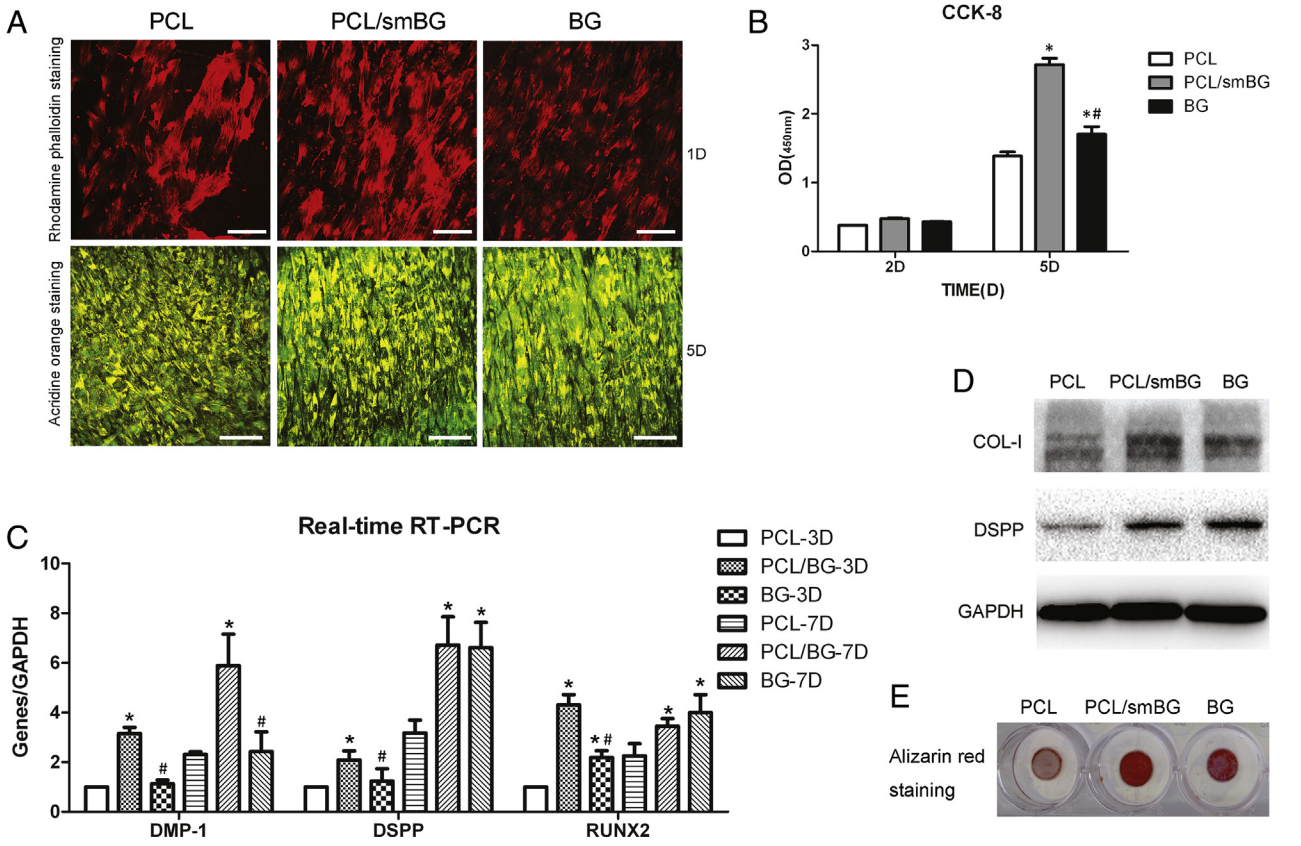

Figure 3. The biological effects of scaffolds on dental pulp cells. (*A*) Immunofluorescence staining of the cytoskeleton of cells (*red*, rhodamine phalloidin staining) and the living cells (yellowish-green, acridine orange staining) (scale bar = 100 μm). (*B*) *In vitro* proliferation of hDPCs on different scaffolds using the Cell Counting Kit-8 test. (*C*) Odontogenic-related gene expression in hDPCs on different scaffolds as assessed by real-time reverse-transcription polymerase chain reaction. DMP-1, dentin matrix protein 1; DSPP, dentin sialophosphoprotein; RUNX2, runt-related transcription factor 2. (*D*) Odontogenic-related protein expression in hDPCs on different scaffolds by Western blot. Col I, collagen I. (*E*) Comparison of the mineralized nodules generated on different scaffolds by alizarin red staining. *Significant differences between the PCL/smBG or BG group and the PCL group ($P < .05$). #Significant differences between the PCL/smBG group and the BG group ($P < .05$).

The biological effects of PCL/smBG composites on dental pulp cells were investigated. All scaffolds showed good cellular responses. The proliferation and odontogenic response of hDPCs to PCL were significantly improved by the addition of smBG particles. In addition, the response was stronger than that obtained with pure 45S5 BG scaffolds. When PCL/smBG hybrids were incubated in SBF, Si^{4+}, Ca^{2+}, and PO_4^{3-}, ions were released into the solution. This was followed by the consumption of the released ions as well as ions in the SBF to form hydroxyapatite layers on the hybrids. The ions released from BG were directly associated with *in vitro* mineralization and enhanced gene expression (16). BG specifically releases Si ions, which are essential to the formation and calcification of mineralized tissue (17, 18) and are thought to play a role in cellular stimulation because of their essential role in bone formation (19). Si ions released from calcium silicate materials promote cell proliferation. In addition, these ions also induce odontoblastic differentiation and mineralization in hDPCs through fibroblast growth factor receptor and extracellular signal-regulated kinase (ERK)/mitogen-activated protein kinases (MAPK) activation (20, 21) and facilitate angiogenic differentiation via the p38 signaling pathway (22). However, different compositional ratios in the scaffold affect the ions in extracts and further affect the microenvironment and cellular responses (23).

Our data showed that the Si concentration in SBF of PCL/smBG composites increased more slowly than with pure BG potentially because the smBG particles in the composite were wrapped by the PCL, which slowed the Si ion release at the initial stage. Later, the mineralization of PCL/smBG was stronger than that of pure BG given the relatively large surface area of smBG. The dose of dissolution products is important for biological activity because too many ions can be toxic (24). The effect on gene expression is dose dependent, and the highest expression was noted with ~20 μg/mL soluble Si (1). A similar dose-dependent response was noted for mature osteoblasts, with 15–20 μg/mL soluble Si promoting the highest metabolic activity, enhanced expression of core-binding factor alpha 1, and the formation of mineralized bone nodules (25). The concentration of ions released by PCL/smBG was lower than that released by pure BG on day 1. The concentration of Si was ~20 μg/mL, which may be more suitable for cell proliferation and differentiation than the other groups. Although the initial adhesive cell was similar, the cell number on PCL/smBG increased more rapidly, and this group had a higher cell number than the other groups on day 5.

Apatite formation on the BG surface is critical for direct bone bonding and may be used as one of the screening criteria for the evaluation of *in vitro* bioactivity of materials. Compared with the pure BG group, apatite that formed on PCL/smBG during the initial days exhibited a more extensive 3-dimensional surface that may provide more adsorptive and bioactive sites and subsequently enhanced protein and growth factor adsorption. These effects aid in subsequent cell

proliferation and differentiation (26, 27). Furthermore, the layer on the PCL/smBG hybrids was thicker on day 5, suggesting that PCL/smBG had stronger mineralization ability than pure BG. The consistent apatite-forming ability of PCL/smBG determined the effectiveness of the cell biological reaction and induced cell mineralization. Scaffolds of varying mechanical properties direct the stem cell lineage (28), but the interactions at the apatite-host interface are less well understood; these mechanisms still require further investigation.

Conclusions

The present study showed that the novel PCL/smBG hybrid scaffold significantly enhances the proliferation and differentiation of hDPCs. The results indicate that PCL/smBG might be a suitable scaffold for tooth engineering. Further research will emphasize the orderly regulation of odontogenic differentiation and pulp regeneration by adjusting the physical and chemical properties of BG composites.

Acknowledgments

The authors thank Dr Iain Bruce for the English language polishing.

Supported by the National Natural Science Foundation of China (51372005).

The authors deny any conflicts of interest related to this study.

References

1. Jones JR. Reprint of: Review of bioactive glass: From Hench to hybrids. Acta Biomater 2015;23(suppl):S53–82.
2. Wang S, Gao X, Gong W, et al. Odontogenic differentiation and dentin formation of dental pulp cells under nanobioactive glass induction. Acta Biomater 2014;10:2792–803.
3. Gong W, Huang Z, Dong Y, et al. Ionic extraction of a novel nano-sized bioactive glass enhances differentiation and mineralization of human dental pulp cells. J Endod 2014;40:83–8.
4. Poh PS, Hutmacher DW, Stevens MM, et al. Fabrication and in vitro characterization of bioactive glass composite scaffolds for bone regeneration. Biofabrication 2013;5:045005.
5. Lei B, Shin KH, Noh DY, et al. Sol-gel derived nanoscale bioactive glass (NBG) particles reinforced poly(epsilon-caprolactone) composites for bone tissue engineering. Mater Sci Eng C Mater Biol Appl 2013;33:1102–8.
6. Filipowska J, Pawlik J, Cholewa-Kowalska K, et al. Incorporation of sol-gel bioactive glass into PLGA improves mechanical properties and bioactivity of composite scaffolds and results in their osteoinductive properties. Biomed Mater 2014;9:065001.
7. Qu T, Liu X. Nano-structured gelatin/bioactive glass hybrid scaffolds for the enhancement of odontogenic differentiation of human dental pulp stem cells. J Mater Chem B Mater Biol Med 2013;1:4764–72.
8. Bae WJ, Min KS, Kim JJ, et al. Odontogenic responses of human dental pulp cells to collagen/nanobioactive glass nanocomposites. Dent Mater 2012;28:1271–9.
9. Hu Q, Chen X, Zhao N, et al. Facile synthesis and in vitro bioactivity of monodispersed mesoporous bioactive glass sub-micron spheres. Mater Lett 2013;106:452–5.
10. Chang SW, Lee SY, Kang SK, et al. In vitro biocompatibility, inflammatory response, and osteogenic potential of 4 root canal sealers: Sealapex, Sankin apatite root sealer, MTA Fillapex, and iRoot SP root canal sealer. J Endod 2014;40:1642–8.
11. Azimi S, Fazlyab M, Sadri D, et al. Comparison of pulp response to mineral trioxide aggregate and a bioceramic paste in partial pulpotomy of sound human premolars: a randomized controlled trial. Int Endod J 2014;47:873–81.
12. Tran D, He J, Glickman GN, et al. Comparative analysis of calcium silicate-based root filling materials using an open apex model. J Endod 2016;42:654–8.
13. Lei B, Chen X, Han X, et al. Unique physical–chemical, apatite-forming properties and human marrow mesenchymal stem cells (HMSCs) response of sol–gel bioactive glass microspheres. J Mater Chem 2011;21:12725–34.
14. Hu Q, Chen X, Zhao N, et al. Fabrication and characterization of dodecylamine derived monodispersed mesoporous bioactive glass sub-micron spheres. J Solgel Sci Technol 2014;69:9–16.
15. Hu Q, Li Y, Miao G, et al. Size control and biological properties of monodispersed mesoporous bioactive glass sub-micron spheres. RSC Adv 2014;4:22678–87.
16. Xynos ID, Edgar AJ, Buttery LD, et al. Gene-expression profiling of human osteoblasts following treatment with the ionic products of Bioglass 45S5 dissolution. Biomed Mater Res 2001;55:151–7.
17. Carlisle EM. Silicon: a requirement in bone formation independent of vitamin D1. Calcif Tissue Int 1981;33:27–34.
18. Carlisle EM. Silicon: an essential element for the chick. Science 1972;178:619–21.
19. Sepulveda P, Jones JR, Hench LL. In vitro dissolution of melt-derived 45S5 and sol-gel derived 58S bioactive glasses. J Biomed Mater Res 2002;61:301–11.
20. Wu BC, Kao CT, Huang TH, et al. Effect of verapamil, a calcium channel blocker, on the odontogenic activity of human dental pulp cells cultured with silicate-based materials. J Endod 2014;40:1105–11.
21. Liu CH, Hung CJ, Huang TH, et al. Odontogenic differentiation of human dental pulp cells by calcium silicate materials stimulating via FGFR/ERK signaling pathway. Mater Sci Eng C Mater Biol Appl 2014;43:359–66.
22. Chou MY, Kao CT, Hung CJ, et al. Role of the P38 pathway in calcium silicate cement-induced cell viability and angiogenesis-related proteins of human dental pulp cell in vitro. J Endod 2014;40:818–24.
23. AbdulQader ST, Kannan TP, Rahman IA, et al. Effect of different calcium phosphate scaffold ratios on odontogenic differentiation of human dental pulp cells. Mater Sci Eng C Mater Biol Appl 2015;49:225–33.
24. Rismanchian M, Khodaeian N, Bahramian L, et al. In-vitro comparison of cytotoxicity of two bioactive glasses in micropowder and nanopowder forms. Iran J Pharm Res 2013;12:437–43.
25. Tsigkou O, Jones JR, Polak JM, et al. Differentiation of fetal osteoblasts and formation of mineralized bone nodules by 45S5 Bioglass conditioned medium in the absence of osteogenic supplements. Biomaterials 2009;30:3542–50.
26. Hench LL, Jones JR. Bioactive glasses: frontiers and challenges. Front Bioeng Biotechnol 2015;3:194.
27. Kingshott P, Andersson G, McArthur SL, et al. Surface modification and chemical surface analysis of biomaterials. Curr Opin Chem Biol 2011;15:667–76.
28. Even-Ram S, Artym V, Yamada KM. Matrix control of stem cell fate. Cell 2006;126:645–7.